Since January 2020 Elsevier has created a COVID-19 resource centre with free information in English and Mandarin on the novel coronavirus COVID-19. The COVID-19 resource centre is hosted on Elsevier Connect, the company's public news and information website.

Analytica Chimica Acta 1212 (2022) 339909

Contents lists available at ScienceDirect

Analytica Chimica Acta

journal homepage: www.elsevier.com/locate/aca

Detection of SARS-CoV-2 RNA through tandem isothermal gene amplification without reverse transcription

Hyojin Lee [a], Hyobeen Lee [a], Sang-Hyun Hwang [b], Woong Jeong [c], Dong-Eun Kim [a,*]

[a] Department of Bioscience and Biotechnology, Konkuk University, 120 Neungdong-ro, Gwangjin-gu, Seoul, 05902, Republic of Korea
[b] Department of Laboratory Medicine, Asan Medical Center, University of Ulsan College of Medicine, Seoul, 05505, Republic of Korea
[c] Department of Emergency Medicine, Kyung Hee University Hospital, Kangdong-gu, Seoul, 05278, Republic of Korea

HIGHLIGHTS

- Fluorometric detection system of SARS-CoV-2 RNA was developed using the tandem isothermal gene amplification (TIGA).
- TIGA assay is composed of rolling circle amplification and strand displacement amplification.
- A stretch of ssDNA containing G-quadruplex was produced with enhanced fluorescence due to thioflavin T intercalation.
- SARS-CoV-2 RNA was sensitively detected with a detection limit of 5.9 aM in 1 h.

GRAPHICAL ABSTRACT

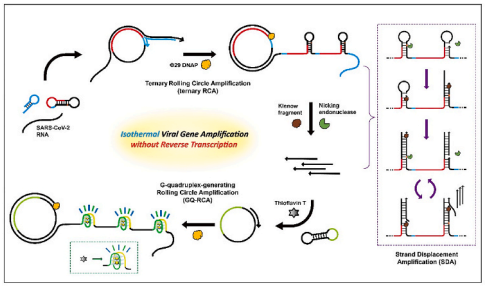

ARTICLE INFO

Keywords:
SARS-CoV-2 viral RNA
Isothermal gene amplification
Rolling circle amplification
Strand displacement amplification
Thioflavin T

ABSTRACT

Diagnosis of SARS-CoV-2 infection through rapid, accurate, and sensitive testing is the most important and fundamental step in coping with the COVID-19 epidemic. We have developed a sensitive fluorometric assay to detect SARS-CoV-2 viral RNA without thermal cycling. This assay system, based on tandem isothermal gene amplification (TIGA), is composed of ternary rolling circle amplification (t-RCA) and subsequent strand displacement amplification (SDA) coupled with G-quadruplex-generating RCA (SDA/GQ-RCA). Without the need to convert viral RNA into cDNA, viral RNA forms a ternary complex composed of hairpin primer (HP) and dumbbell padlock DNA during the t-RCA process. t-RCA generates a long chain of single-stranded DNA (ssDNA) with tandemly repeated hairpin structures that are subjected to SDA. SDA produces multiple short ssDNAs from t-RCA products, which then serve as primers for the second RCA reaction. A long ssDNA harboring repeated copies of the G-quadruplex is produced in the second round of RCA. Emission of enhanced fluorescence by thioflavin T, which intercalates into the G-quadruplex, allows fluorometric detection of amplified viral genes. This fluorometric analysis sensitively detected SARS-CoV-2 RNA as low as 5.9 aM, with a linear range between 0.2 fM and 200 fM within 1 h. Hence, this isothermal gene amplification method without reverse transcription of viral RNA can be applied to diagnose COVID-19 with high sensitivity and accuracy as an alternative to current PCR-based diagnosis.

* Corresponding author. Department of Bioscience and Biotechnology, Konkuk University, Gwangjin-gu, Seoul, 05029, Republic of Korea.
E-mail address: kimde@konkuk.ac.kr (D.-E. Kim).

https://doi.org/10.1016/j.aca.2022.339909
Received 3 February 2022; Received in revised form 27 April 2022; Accepted 3 May 2022
Available online 6 May 2022

1. Introduction

Coronavirus disease 2019 (COVID-19) is an infectious respiratory disease caused by severe acute respiratory syndrome coronavirus 2 (SARS-CoV-2) [1,2]. To cope with the current worldwide COVID-19 epidemic, the detection of SARS-CoV-2 through rapid, accurate, and sensitive testing is essential. Nucleic acid testing is considered a feasible and practical method for the diagnosis of SARS-CoV-2, in which nucleic acid amplification is employed to detect small amounts of viral RNA [3,4]. Currently, most countries diagnose COVID-19 infections by detecting SARS-CoV-2 RNA via reverse transcription quantitative real-time PCR (RT-qPCR) [5,6], in which fluorescent signals are monitored during each cycle of the PCR amplification process in order to analyze template presence and abundance. For RT-qPCR-based testing for SARS-CoV-2 diagnosis, the viral RNA is first reverse-transcribed into cDNA for the PCR amplification of target marker genes (e.g., *ORF1ab/RdRp*, *E*, and *N* genes) [6,7].

Standard RT-qPCR methods that require laboratory-based testing instruments such as a thermal cycler for DNA amplification have constraints, including high cost, detection time, and the need for trained experts, limiting their application in point-of-care (POC) testing and resource-limited areas [8–10]. To overcome these limitations, isothermal amplification methods have emerged as alternatives to PCR-based technologies, including loop-mediated isothermal amplification (LAMP) [11], recombinase polymerase amplification (RPA) [12], strand displacement amplification (SDA) [13], and rolling circle amplification (RCA) [14]. The isothermal gene amplification method is attractive because amplification of the target genetic material is performed at a constant temperature. In addition to this advantage, the isothermal amplification method is appropriate for POC testing to meet the urgent need for viral diagnosis to be performed outside of a laboratory, with great market demand for portable nucleic acid amplification analyzers. Especially, SDA has been used as a method combined with other isothermal gene amplification tools to detect target genes. In the SDA process, target nucleic acid is amplified using nicking endonuclease (NE) and a strand-displacing DNA polymerase, such as the exonuclease-deficient Klenow fragment (KF) [15,16]. NE produces a nick by cutting one strand of the target dsDNA at its recognition site, and KF DNA polymerase subsequently extends the DNA from the 3′-end of the nick and displaces the downstream strands. The displaced ssDNAs that were amplified through SDA process can be subsequently utilized as primers or templates in downstream workflow [17–19].

Multitude of groups have developed target gene detection methods based on isothermal gene amplification utilizing RCA, one of the robust isothermal amplification tools, which were widely implicated in the detection of DNA and RNA (miRNA, mRNA, and viral RNA) [20–22]. The RCA process utilizes a circular padlock DNA template and strand-displacing DNA polymerase, such as phi29 DNA polymerase, by which long ssDNA possessing repeated sequences are efficiently synthesized. Most of RCA-based target gene detection methods depend on ligation of a linear padlock DNA with splint target nucleic acid sequences, which is a critical target decision step. However, this ligation step is presumably rate-limiting because annealing of the target sequences to the padlock DNA is often unlikely due to low concentration of target molecule, self-structured nucleic acids, or non-specific binding. Especially, the ligation-based RCA has limitations in application to direct detection of long RNAs (>3000 nucleotides; nt), such as viral RNA [23,24]. Several attempts have been made to modify the padlock DNA or the RCA process to overcome difficulties in the ligation of padlock DNA. These include use of pre-ligated circular padlock DNA, ternary primer that binds to both target molecules and padlock DNA to form a ternary complex [25,26], hairpin probe-based RCA (HP-RCA) [27,28], and primer generation-RCA (PG-RCA) [29,30]. Although each method has demonstrated usefulness in the detection of target genes, these have not been fully successful in the detection of long RNAs with a satisfactory signal-to-background ratio (S/B ratio). Thus, it is necessary to combine the merits of these modified RCA methods to enable isothermal amplification of viral RNA present in samples.

Our group previously developed a fluorometric method for detecting the RCA-amplified DNAs using G-quadruplex formation with a fluorescence enhancement system (GQ-RCA) [31,32]. In this fluorometric detection method, G-quadruplexes formed in the RCA products were intercalated with thioflavin T (ThT), which emits enhanced fluorescence due to the restricted free rotation of ThT in the DNA structure. Using the fluorometric method for detecting RCA-amplified DNAs, we previously developed methods for detection of influenza viral genes; the pre-ligated circular padlock DNA and hairpin probe DNA were used for recognition of target nucleic acid sequence, comprising the ternary initiation complex in the RCA (i.e., ternary RCA) [33], and the primer generating SDA coupled RCA [34]. Despite the merits of these modified RCA methods, the conversion of viral RNA into cDNA by reverse transcription for subsequent PCR amplification of viral genes was unavoidable before the RCA process.

In this study, we developed an isothermal gene amplification system for SARS-CoV-2 viral RNA detection by tandemly combining isothermal gene amplification tools without the need for reverse transcription of RNA into cDNA. Our tandem isothermal gene amplification (TIGA) method consists of ternary RCA (t-RCA) and subsequent SDA coupled with GQ-RCA (SDA/GQ-RCA). In the presence of target SARS-CoV-2 viral RNA, the t-RCA process generated ssDNA products containing the NE recognition sequence, which were subjected to SDA using NE and KF. The multiple ssDNAs generated through SDA were used as primers for the subsequent isothermal gene amplification process (GQ-RCA). SDA and GQ-RCA were carried out in the same tube (i.e., one-pot assay) without thermal cycling, resulting in the emission of strong fluorescence by ThT intercalated into the tandem repeats of the G-quadruplex. This fluorometric isothermal viral RNA detection system can be used to quantitatively detect long SARS-CoV-2 RNA with high sensitivity, accuracy, and convenience in resource-limited areas and in POC testing.

2. Material and methods

2.1. Viral RNAs, DNA oligonucleotides, enzymes, and chemical reagents

Pathogens (viral RNAs from SARS-CoV-2: NCCP43329, NCCP43331, and NCCP43326) for this study were provided by the National Culture Collection for Pathogens (Korea Disease Control and Prevention Agency, Cheongju, Korea). SARS-CoV-2 (omicron variants) RNAs from patients, which were approved by the Ethical Review Board of the Asan Medical Center (IRB No. 2020–1532), and hepatitis C virus RNAs were provided by the Asan Medical Center (Seoul, Korea). Samples of influenza virus RNA (influenza A virus/California/07/2009/H1N1, GenBank No. NC026433.1; influenza A virus/Texas/50/2012/H3N2, GenBank No. KC892952.1; influenza B/Massachusetts/02/2012/Yamagata lineage, GenBank No. KC892118.1) were provided by the Korea Institute of Radiological and Medical Science (Seoul, Korea). DNA oligonucleotides used for isothermal gene amplification (RCA and SDA) were chemically synthesized and purified by high-performance liquid chromatography (Bionics, Seoul, Korea). Detailed DNA sequences are shown in Table S1. T7 RNA polymerase, recombinant RNase inhibitor, recombinant DNase I, *Taq* DNA polymerase (*Ex Taq*®), exonuclease I, exonuclease III, T4 DNA ligase, and dNTPs were purchased from Takara Korea Biomedical, Inc. (Seoul, Korea). Phi29 DNA polymerase, Klenow fragment (exo-), and nicking endonuclease (Nb.BbvCI) were purchased from New England Biolabs (Ipswich, MA, USA). Thioflavin T was purchased from Sigma-Aldrich (St. Louis, MO, USA). EtBr and SYBR gold staining dyes were purchased from Invitrogen (Carlsbad, CA, USA). qPCR RT Master Mix (ReverTra Ace®) was purchased from Toyobo (Osaka, Japan). rCTP, rGTP, rUTP, and rATP (100 mM each) were purchased from Promega (Madison, WI, USA). Rotor Gene SYBR® Green PCR kit was purchased from Qiagen (Hilden, Germany). The pooled normal human plasma was purchased from Innovative Research (Novi, MI, USA).

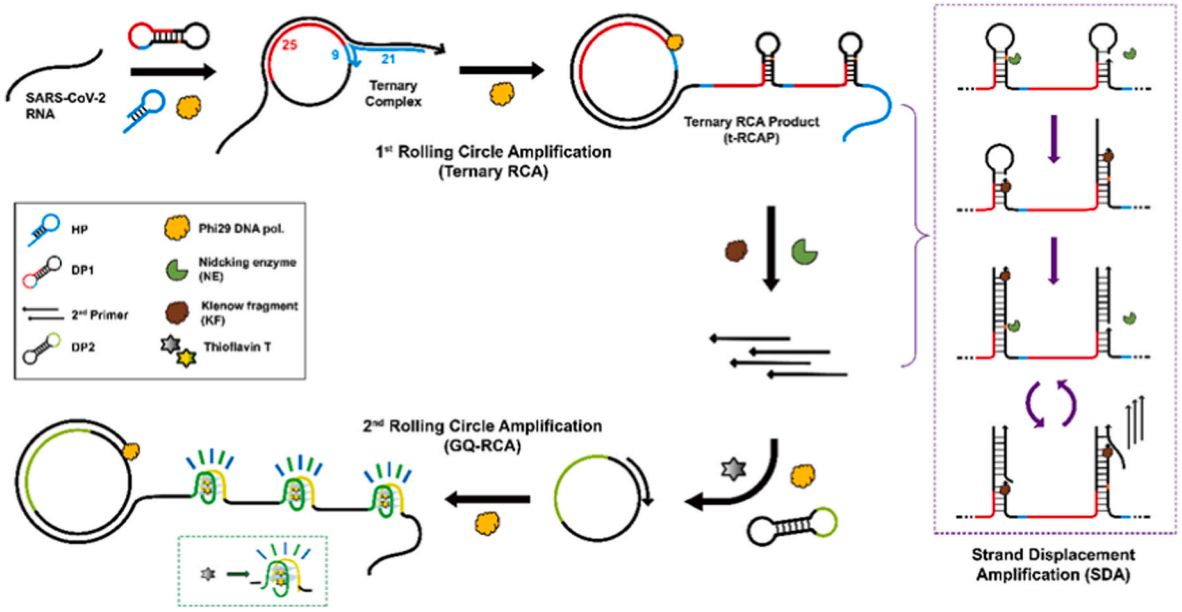

Scheme 1. Schematic illustration of tandem isothermal gene amplification for fluorometric detection of SARS-CoV-2 viral RNA.

2.2. *In vitro synthesis of SARS-CoV-2 RdRp RNA*

To prepare SARS-CoV-2 *RdRp* RNA as the target analyte RNA, cDNA was first synthesized from SARS-CoV-2 viral RNA using the qPCR RT Master Mix (ReverTra Ace®) according to the manufacturer's protocol. PCR was carried out with 25 μL of a reaction mixture containing 2 μL of cDNA, 2.5 U *Taq* DNA polymerase (*Ex Taq*®, Takara), and PCR primers (*RdRp* forward and reverse primers; 200 nM each; Table S1) under the following conditions: pre-denaturation at 95 °C for 2 min, 35 cycles of 30 s denaturation at 95 °C, 30 s primer annealing at 58 °C, and 30 s extension at 72 °C, and final incubation at 72 °C for 5 min. After PCR amplification of *RdRp*, 2.5 μL of the PCR products was mixed in 50 μL reaction solution containing 1 × T7 RNA polymerase buffer (50 mM Tris-HCl, 15 mM $MgCl_2$, 20 mM spermidine, and 5 mM DTT; pH 7.5), 2 mM dNTP mixture, 100 U T7 RNA polymerase, and 40 U recombinant RNase inhibitor. The reaction mixture was incubated at 37 °C for 2 h, and then 5 U DNase I was added for DNA degradation. After incubation at 37 °C for 15 min, 20 mM EDTA was added to the reaction mixture to arrest the enzymatic reactions. *In vitro* synthesized *RdRp* RNA (285 nt) was purified by a gel extraction method [35] using denaturing polyacrylamide gel (6%) electrophoresis with 8 M urea (urea-PAGE). The concentration of purified RNA was measured using a UV–Vis spectrophotometer (Ultrospec 2100 pro spectrophotometer; Biochrom Ltd, Cambridge, UK) at a wavelength of 260 nm.

2.3. *Preparation of ligated dumbbell padlock DNAs*

To ligate two termini of dumbbell padlock DNAs (DP1 or DP2), 10 μL of a reaction mixture containing 3 μM 5′-phosphorylated linear dumbbell padlock DNA (DP1 or DP2), 175 U of T4 DNA ligase, and 1 × T4 DNA ligase buffer (66 mM Tris-HCl, 6.6 mM $MgCl_2$, 10 mM DTT, and 0.1 mM ATP; pH 7.6) was incubated at 22 °C for 1 h. To degrade non-ligated linear padlock DNAs, the reaction mixture was supplemented with 5 μL of a mixture containing 15 U of exonuclease I, 100 U of exonuclease III, and 1 × exonuclease I buffer (67 mM glycine-KOH, 6.7 mM $MgCl_2$, 1 mM DTT; pH 9.5) and incubated at 37 °C for 2 h. The reaction was terminated by heating the mixture at 95 °C for 10 min. The ligated and exonuclease-treated products were analyzed via urea-PAGE (10%) and visualized using a UV transilluminator after staining with SYBR Gold. The resulting reaction aliquot was used as dumbbell padlock DNA in a closed form for subsequent RCA reactions.

2.4. *RCA reaction with dumbbell padlock DNA and HP: t-RCA*

The target sequence in *RdRp* RNA (5 ng) was amplified by RCA with pre-ligated dumbbell padlock DNA and HP for t-RCA. The reaction mixture (25 μL) contained 200 nM of the 1st dumbbell padlock DNA (DP1), 500 μM dNTPs, 200 nM HP, 1 × phi29 DNA polymerase buffer (50 mM Tris-HCl, 10 mM $MgCl_2$, 10 mM $(NH_4)_2SO_4$, and 4 mM DTT; pH 7.5), and 115 U phi29 DNA polymerase. The ternary RCA mixture was incubated at 32 °C for 30 min, followed by heat-inactivation at 65 °C for 10 min. t-RCA products (t-RCAP) were analyzed by urea-PAGE (10%) and visualized using a UV transilluminator after staining with SYBR Gold.

2.5. *SDA-coupled RCA with G-quadruplex-based fluorescence enhancement: SDA/GQ-RCA*

The one-tube SDA/GQ-RCA reaction mixture (25 μL) contained an aliquot of t-RCA products (2.5 μL of 25 μL preceding RCAP), 500 μM dNTPs, 100 nM of the 2nd dumbbell padlock DNA (DP2), 2.5 U KF, 10 U Nb.BbvCI, 115 U phi29 DNA polymerase, and 15 μM ThT in a reaction buffer (50 mM potassium acetate, 20 mM Tris-acetate, 10 mM magnesium acetate, 100 μg/ml BSA, and 2 mM KCl; pH 7.9). The reaction mixture was incubated at 32 °C for 30 min, and the reaction was terminated by heating at 95 °C for 10 min. To visualize the enhanced ThT fluorescence due to ThT intercalation into the G-quadruplex, the heat-quenched reaction products in a transparent PCR tube, after cooling at 8 °C for 5 min, were photographed under UV illumination using a PowerShot A640 digital camera (Canon Inc., Tokyo, Japan). The fluorescence intensity of each reaction sample (25 μL) containing ThT intercalated into the G-quadruplex, which was diluted with the same volume of double-distilled water, was measured using a fluorescence spectrophotometer (Cary Eclipse, Agilent Technologies, Santa Clara, CA, USA); $\lambda_{ex} = 425$ nm and $\lambda_{em} = 488$ nm; PMT voltage = 600.

2.6. *Detection of SARS-CoV-2 full-length RNA with TIGA assay*

Fifty nanograms of SARS-CoV-2 full-length RNA (~30,000 nt) or clinical samples obtained from SARS-CoV-2 positive patients (1.0 μL) was used as the target analyte RNA for t-RCA (volume: 25 μL) as described in Section 2.4 (*RCA reaction with dumbbell padlock DNA and HP: t-RCA)*. An aliquot of t-RCA products (2.5 μL) was subsequently used

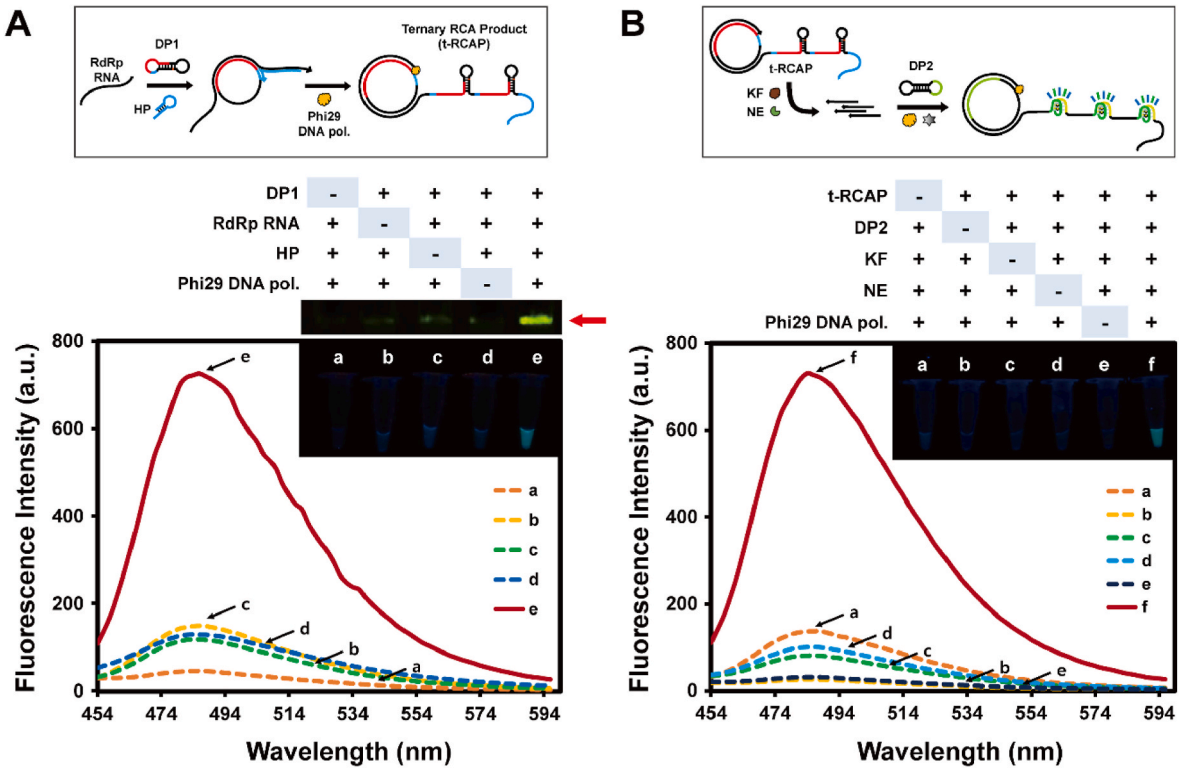

Fig. 1. Evaluation of tandem isothermal gene amplification with ThT fluorescence enhancement. (A) Evaluation of the ternary RCA (scheme shown above) with electrophoretic analysis (urea-PAGE, 10%) of amplified ssDNA and subsequent ThT fluorescence enhancement under various t-RCA conditions: a, without the 1st dumbbell padlock DNA (DP1); b, without target RNA (*RdRp* RNA); c, without hairpin primer (HP); d, without phi29 DNA polymerase; e, all included. Fluorescent gel image was visualized under UV light after SYBR Gold staining of amplified DNA (shown by arrow). ThT fluorescence enhancement resulting from the subsequent SDA/GQ-RCA reaction under various t-RCA conditions (a ~ e) was measured at an excitation wavelength (λ_{ex}) of 425 nm with a scanning of emission wavelengths. (B) Evaluation of the SDA/GQ-RCA reaction (scheme shown above) using the DNA amplified with the preceding t-RCA under various SDA/GQ-RCA conditions: a, without the t-RCA product (t-RCAP); b, without the 2nd dumbbell padlock DNA (DP2); c, without the Klenow fragment (KF); d, without the nicking endonuclease (NE); e, without phi29 DNA polymerase; f, all included. Fluorescence emission spectra (λ_{ex} = 425 nm) of ThT intercalated into the SDA/GQ-RCA products under various conditions were obtained as described in (A). Each sample used for fluorescence measurements was visualized under UV light (inset image).

in the SDA/GQ-RCA reaction, which was performed as described in Section 2.5 (*SDA-coupled RCA with G-quadruplex-based fluorescence enhancement: SDA/GQ-RCA*). The resulting ThT fluorescence was measured using a fluorescence spectrophotometer, as described in Section 2.5. For the spike-and-recovery test, varying amounts of SARS-CoV-2 full-length RNA (240 pg, 2.4 ng, and 24 ng) were spiked into the pooled normal human plasma (1%) and subjected to tandem isothermal gene amplification according to the same procedures as describe above.

2.7. Reverse transcription quantitative real-time PCR (RT-qPCR)

For quantitative real-time PCR of SARS-CoV-2 RNA, cDNA was first synthesized from several RNA samples, such as *in vitro* synthesized SARS-CoV-2 *RdRp* RNA at varying concentration (200 pM–20 fM), SARS-CoV-2 full-length viral RNA at varying amounts, or clinical samples containing SARS-CoV-2 viral RNAs, using ReverTra Ace® qPCR RT Master Mix, according to the manufacturer's protocol. RT-qPCR was then performed using the Rotor Gene SYBR® Green PCR kit in 25 μL reaction volumes containing 1 × Rotor-Gene SYBR Green PCR master mix, 1 μL of cDNA, and PCR primers (*RdRp* forward and reverse primers; 200 nM each; Table S1) in a real-time thermocycler Rotor Gene Q system (Qiagen) under the following conditions: pre-denaturation at 95 °C for 5 min, followed by 40 cycles of incubation for 30 s at 95 °C, incubation for 30 s at 58 °C, incubation for 30 s at 7 °C, and final extension at 72 °C for 5 min.

3. Results and discussion

3.1. Tandem isothermal gene amplification from viral RNA without reverse transcription

The underlying principle of the TIGA assay for fluorometric detection of SARS-CoV-2 viral RNA is illustrated in Scheme 1. The system comprises two steps: i) t-RCA and ii) SDA coupled with GQ-RCA (SDA/GQ-RCA). The HP has a stem-loop structure, in which the stem structure is self-annealed to prevent binding to the dumbbell padlock DNA in the absence of target viral RNA. Target RNA annealing to the HP induces unfolding of the stem in the HP, which causes better binding of target RNA to the HP due to higher binding affinity than the stem structure in HP; the duplex length (21 bp) of the stem structure composed of HP and target RNA is more than that of the self-annealed stem in the HP (9 bp). Unfolding of the HP annealed to the target RNA provides a binding region for the complementary DP1, resulting in the formation of a ternary complex consisting of HP, target RNA, and DP1. Phi29 DNA polymerase synthesizes long stretches of ssDNA by elongating the 3′-terminus of HP as a primer in the ternary complex. The long stretch of the ssDNA product as the RCA continues (referred to as t-RCA product) contains multiple-repeated hairpin structures that have a recognition sequence for the NE. The t-RCAPs encounter NE and DNA polymerase (KF) for SDA, in which multiple oligonucleotide-DNAs (22-mer), as primers for the subsequent 2nd RCA, are produced by the repeated action of NE and

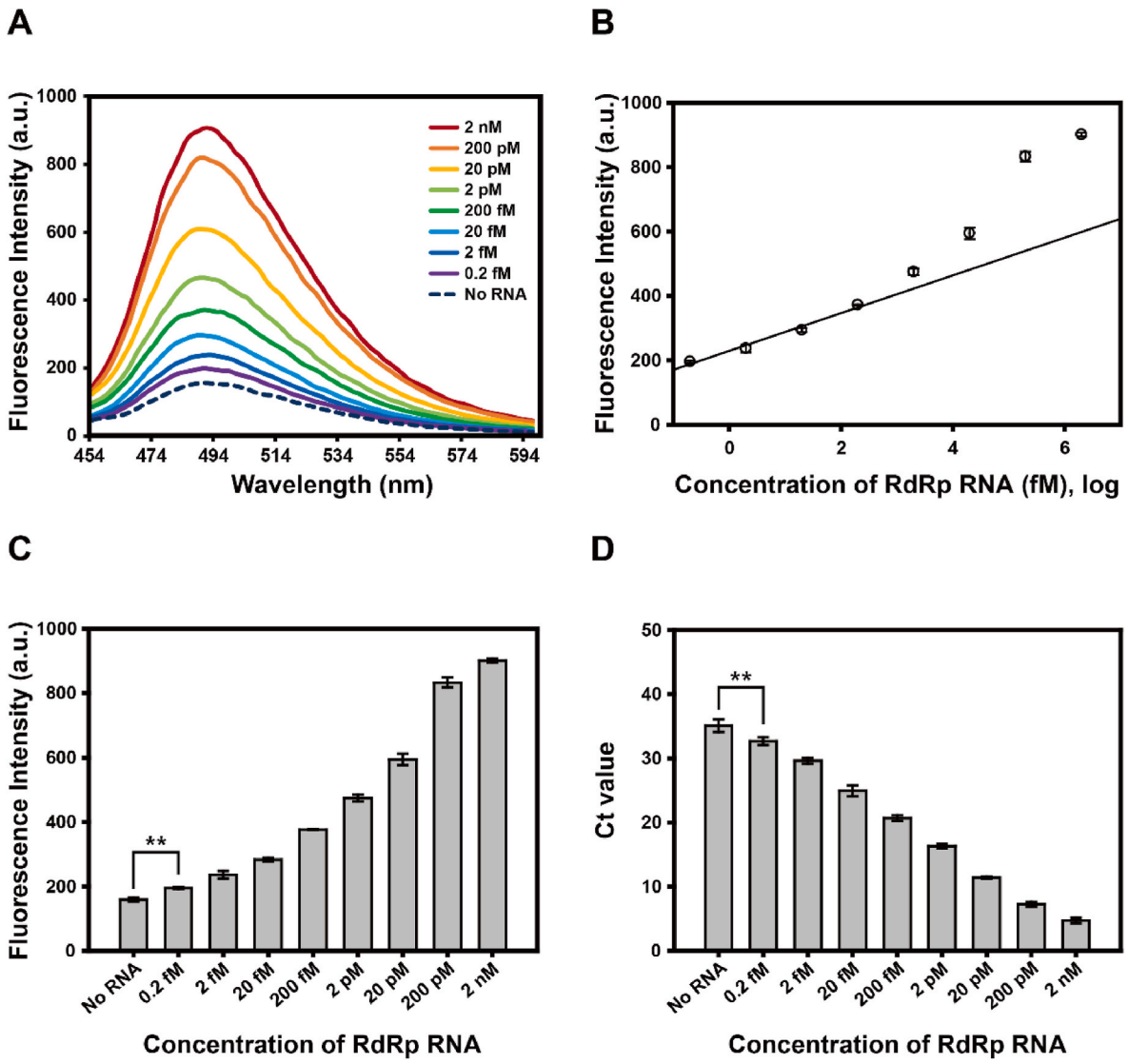

Fig. 2. Sensitivity of the tandem isothermal gene amplification system for the detection of SARS-CoV-2 *RdRp* RNA. (A and B) Viral *RdRp* RNA at increasing concentrations (ranging from 0.2 fM to 2 nM) were tested for fluorometric detection with t-RCA and subsequent SDA/GQ-RCA with ThT fluorescence enhancement. Fluorescence emission spectra ($\lambda_{ex} = 425$ nm) of ThT were scanned (panel A), and the maximal fluorescence intensity obtained at a wavelength of 488 nm was plotted as a function of *RdRp* concentration (panel B). Fluorescence intensity reveals a linear correlation with *RdRp* RNA concentration in the range 0.2 fM to 200 fM (linear line) with an LOD value of 5.9 aM. (C) The bar graph represents the maximal fluorescence intensity ($\lambda_{em} = 488$ nm) obtained by tandem isothermal gene amplification assay for the detection of the target *RdRp* RNA at various concentrations. The assay revealed a statistically significant detection of *RdRp* RNA, at a concentration as low as 0.2 fM (**, $P < 0.01$ vs. no RNA). (D) Conventional RT-qPCR analysis for *RdRp* RNA at various concentrations. The bar graph represents the Ct values obtained during RT-qPCR at different concentrations of SARS-CoV-2 *RdRp* RNA. Positive detection of *RdRp* RNA was achieved at a concentration as low as 0.2 fM and with statistical significance (**, $P < 0.01$ vs. no RNA). Data are presented as means ± standard deviation values obtained from three replicate experiments.

KF on the t-RCAP. As the RCA primers anneal to the DP2, phi29 DNA polymerase initiates the 2nd RCA to generate a long stretch of ssDNA containing multiple repeated G-quadruplex structures that can be intercalated by the fluorophore ThT (i.e., GQ-RCA). The G-quadruplex–ThT complex emits strong fluorescence, which allows this system to quantitatively identify the presence of target viral RNA.

3.2. Validation of tandem isothermal gene amplification

To test our strategy for the fluorometric detection of SARS-CoV-2 viral RNA, we evaluated each step of the TIGA system using SARS-CoV-2 *RdRp* RNA (i.e., *in vitro*-synthesized RNA, 285 nt). First, we prepared the closed form of dumbbell padlock DNAs (DP1 and DP2) used in the tandem RCA procedure by ligation of each end without splint DNA, after which exonuclease treatment confirmed the formation of the closed form of each padlock DNA (Fig. S1). We then examined the validity of target gene amplification by monitoring ssDNA and subsequent ThT fluorescence enhancement under various t-RCA conditions, in which each component of t-RCA was excluded from the required reagents one-by-one with comparison to a positive control ('all included' in Fig. 1A). When the isothermally amplified gene product generated with t-RCA (i.e., t-RCAP) was analyzed by gel electrophoresis, only t-RCAPs of the positive control were retained in the gel well, as the amplified gene had long-stretches of ssDNA. This result indicated that the target RNA was annealed to circular dumbbell padlock DNA (DP1) and an HP to form a ternary complex that enabled the synthesis of long ssDNA as a t-RCAP. The presence of accumulated t-RCAP was confirmed by ThT fluorescence enhancement, which was carried out by the SDA/GQ-RCA reaction with an aliquot of the t-RCAP under various t-RCA conditions (graph in Fig. 1A). The exclusion of any reagent required for t-RCA failed to enhance ThT fluorescence (lines a-d, Fig. 1A), whereas ThT fluorescence was highly enhanced in the positive control (line e,

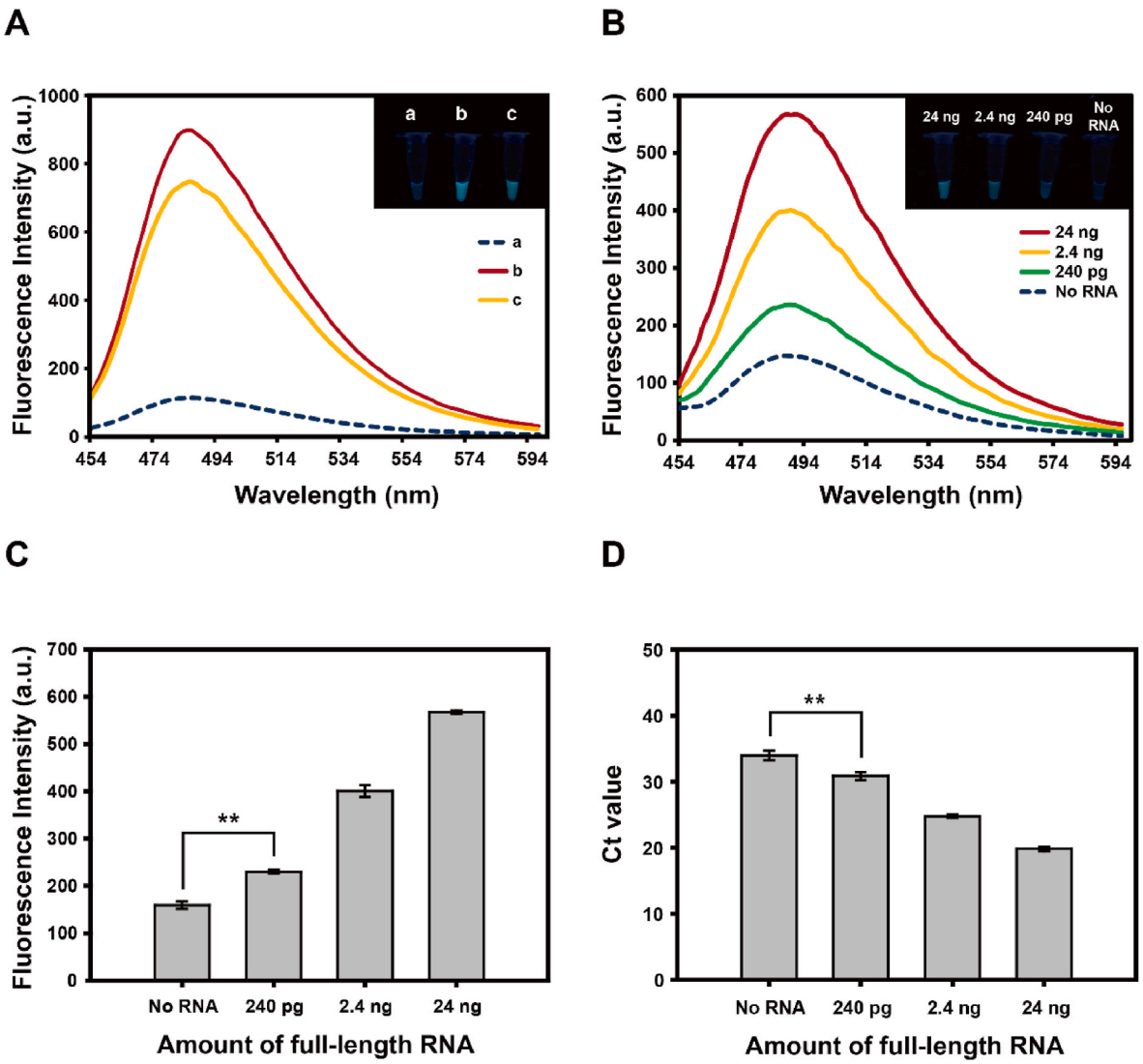

Fig. 3. Fluorometric detection of SARS-CoV-2 full-length RNA with the tandem isothermal gene amplification assay. (A) Both SARS-CoV-2 full-length RNA and *RdRp* RNA were subjected to the fluorometric assay using tandem isothermal gene amplification. Enhanced ThT fluorescence emission ($\lambda_{ex} = 425$ nm) was detected with both viral RNAs; a, RNA-free sample (no RNA); b, *RdRp* RNA (285 nt, 200 pM); c, SARS-CoV-2 full-length RNA (30000 nt, 200 pM). (B) Fluorescence emission spectra ($\lambda_{ex} = 425$ nm) of ThT were obtained with different amounts of SARS-CoV-2 full-length RNA (ranging from 240 pg to 24 ng) that were subjected to tandem isothermal gene amplification. Fluorescence of each sample was visualized under UV light after the measurement of fluorescence (inset image). (C) Each bar graph represents the maximal fluorescence intensity ($\lambda_{em} = 488$ nm) for the detection of full-length SARS-CoV-2 RNA at decreasing amounts. The fluorometric assay detected SARS-CoV-2 full-length RNA at an amount as low as 240 pg, with statistical significance (**, $P < 0.01$ vs. no RNA). (D) Quantitative real-time PCR for detection of SARS-CoV-2 full-length RNA at decreasing amounts. The bar graph representing Ct values obtained during RT-qPCR shows statistically significant positive detection of as low as 240 pg of SARS-CoV-2 full-length RNA (**, $P < 0.01$ vs. no RNA). Data are presented as means ± standard deviation values obtained from three replicate experiments.

Fig. 1A) with green fluorescence visualized under UV illumination (inset in Fig. 1A).

Next, we evaluated the validity of each component in the second part of our detection system, the SDA/GQ-RCA. After the SDA/GQ-RCA reaction using the gene amplified with the preceding t-RCA was performed under various conditions, in which each component of the SDA/GQ-RCA reaction was excluded one-by-one, ThT fluorescence enhancement was measured (graph in Fig. 1B). As expected, ThT fluorescence was greatly enhanced when SDA/GQ-RCA was performed with all reagents (line f, Fig. 1B). However, exclusion of any one component did not result in fluorescence enhancement (lines a-e, Fig. 1B), indicating that the detection of target viral RNA with the TIGA process requires all components of DNA as well as the enzymes in the proposed scheme. The positive signal of enhanced ThT fluorescence, representing the presence of target viral RNA, was compared with the background fluorescence obtained in the absence of target RNA (i.e., S/B). To achieve a maximal S/B, we optimized various experimental conditions such as reaction time, temperature, concentration of enzymes, and concentration of oligo DNAs (Fig. S2). After the optimization, the fluorescence difference in the presence and absence of analyte RNA was estimated to be approximately 6.9 as S/B in the TIGA process with ThT fluorescence enhancement (Fig. S3).

3.3. Sensitivity of fluorometric RNA detection of tandem isothermal gene amplification

To evaluate the sensitivity of fluorometric detection of viral RNA with the TIGA system, serially diluted SARS-CoV-2 *RdRp* RNA (2 nM–0.2 fM) was used to detect ThT fluorescence intensity after TIGA assay (Fig. 2A). The maximal fluorescence of enhanced ThT fluorescence

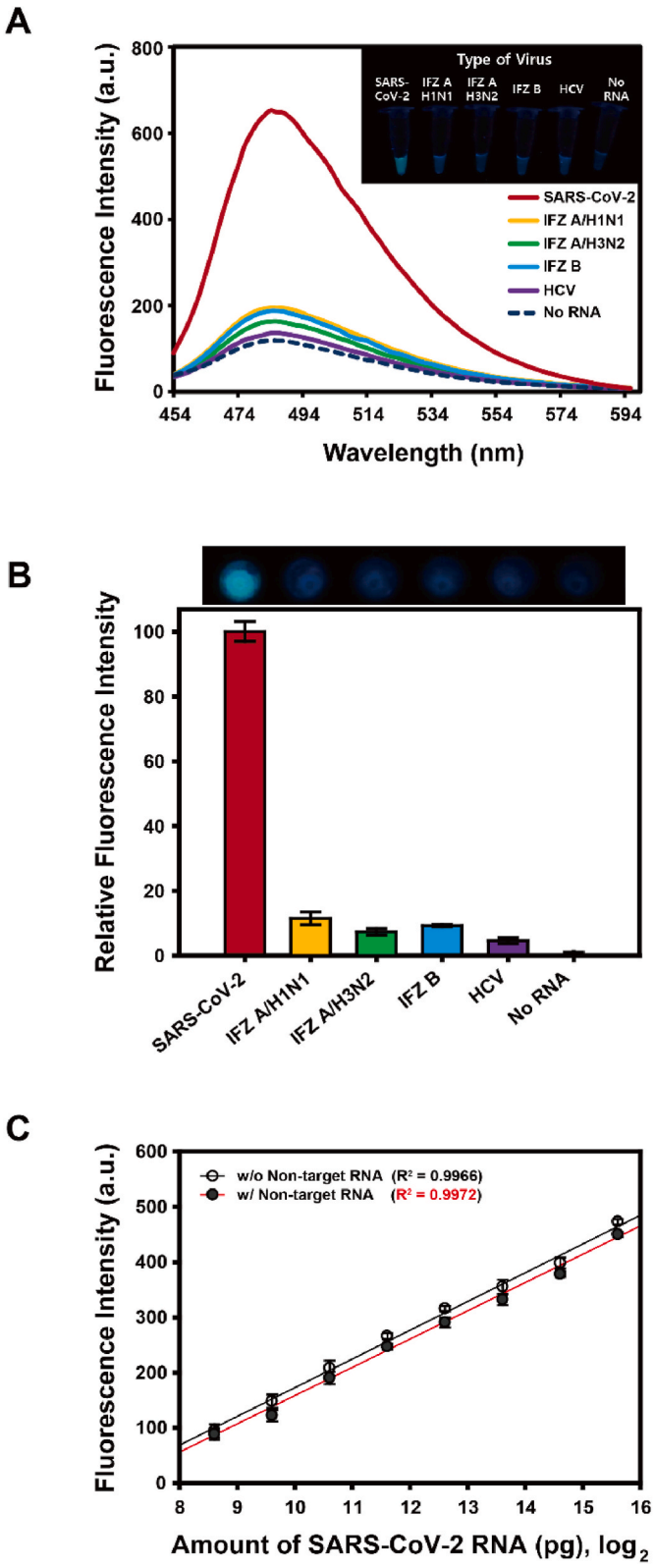

Fig. 4. Selectivity of the fluorometric assay with tandem isothermal gene amplification. ThT fluorescence was monitored after the tandem isothermal gene amplification assay for detection of various RNA viruses using each viral RNA (50 ng) as a sample. (A) Fluorescence emission spectra ($\lambda_{ex} = 425$ nm) were obtained with different types of viral RNA. Each tube containing a viral RNA sample was fluorescently visualized under UV light after fluorescence measurements (inset image). (B) The bar graph shows the fluorescence intensity ($\lambda_{em} = 488$ nm) obtained for each viral RNA sample, which was normalized to values between the target SARS-CoV-2 RNA (100%) and RNA-free sample (zero, no RNA). (C) In the presence or absence of non-target viral RNAs (IFZ A/H1N1, IFZ A/H3N2, and IFZ B; 150 ng in total), target SARS-CoV-2 viral RNA at increasing concentrations (ranging from 390 pg to 50 ng) were tested for TIGA assay. ThT fluorescence intensity obtained at 488 nm as a function of SARS-CoV-2 RNA amount shows a linear correlation with amount of target SARS-CoV-2 RNA regardless of the presence or absence of non-target viral RNA (linear line). Data are presented as means ± standard deviation values obtained from three replicate experiments.

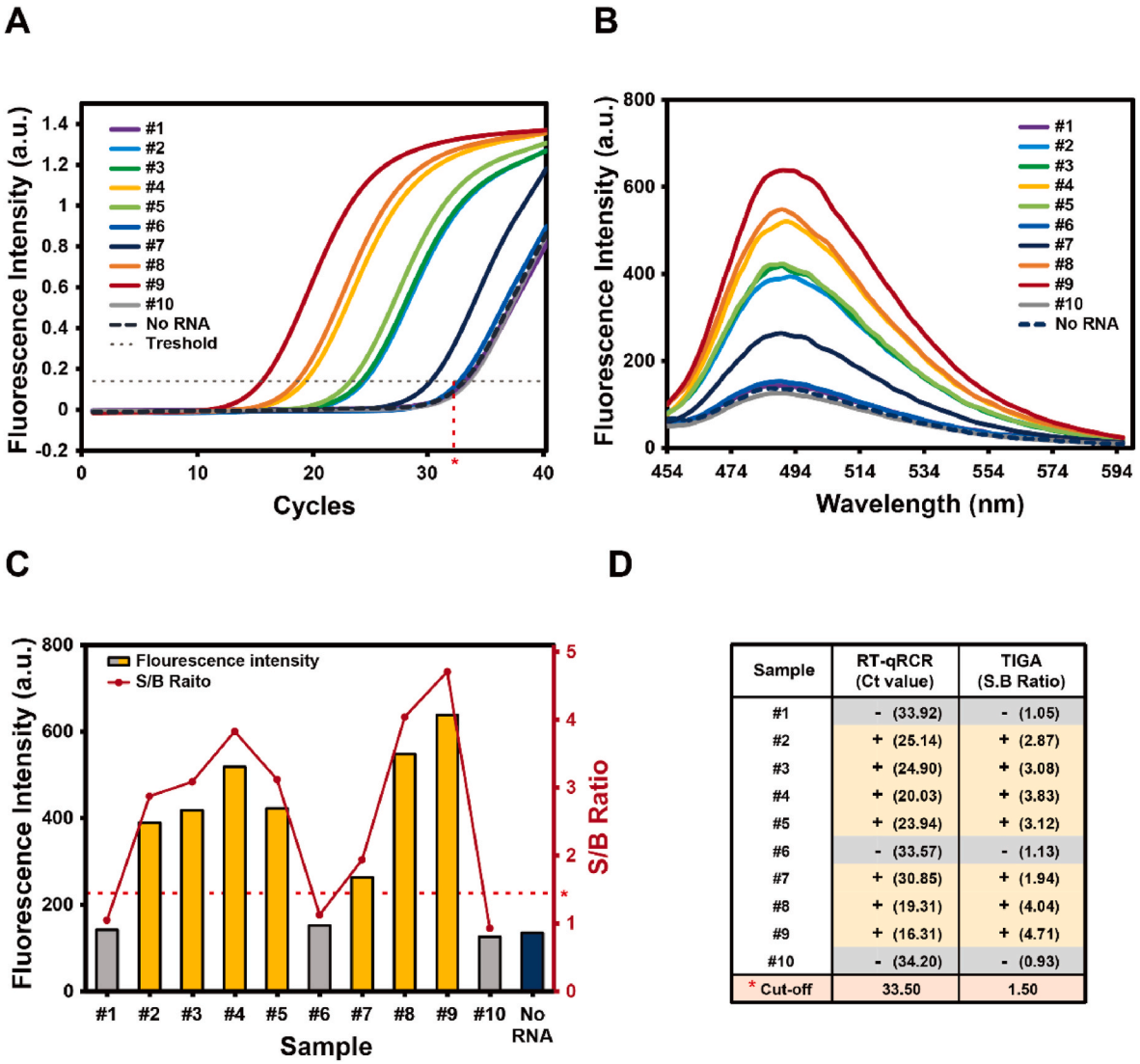

Sample	RT-qRCR (Ct value)	TIGA (S.B Ratio)
#1	- (33.92)	- (1.05)
#2	+ (25.14)	+ (2.87)
#3	+ (24.90)	+ (3.08)
#4	+ (20.03)	+ (3.83)
#5	+ (23.94)	+ (3.12)
#6	- (33.57)	- (1.13)
#7	+ (30.85)	+ (1.94)
#8	+ (19.31)	+ (4.04)
#9	+ (16.31)	+ (4.71)
#10	- (34.20)	- (0.93)
* Cut-off	33.50	1.50

Fig. 5. Evaluation of tandem isothermal gene amplification (TIGA) system for detecting SARS-CoV-2 viral RNA in clinical samples. (A) Curves of fluorescence changes in conventional RT-qPCR analysis with a total of 10 clinical samples including SARS-CoV-2 omicron positive and negative samples. A SARS-CoV-2 positive sample was identified with a threshold cut (dashed line) with Ct value of 33.5 cycles or less (asterisk in the graph). (B) Fluorescence emission spectra ($\lambda_{ex} = 425$ nm) of the same 10 clinical samples were obtained with TIGA assay. (C) The bar graph represents the maximal fluorescence intensity ($\lambda_{em} = 488$ nm) obtained from the 10 clinical samples (shown in panel B). Red dot with line represents signal to background ratio (S/B) obtained by dividing the fluorescence intensity of sample by the background fluorescence obtained in the absence of RNA. The sample with 1.5 or higher S/B (dashed line and asterisk) was classified as SARS-CoV-2 positive cases (orange-colored bars). (D) Table shows a comparison of analysis results obtained with the RT-qPCR and the TIGA method for 10 clinical samples. Three samples (#1, #6, and #10) were determined to be SARS-CoV-2 negative and the rest samples were classified as SARS-CoV-2 positive in both methods.

at 488 nm showed a linear correlation ($R^2 = 0.9916$) with RNA concentration ranging from 0.2 fM to 200 fM (Fig. 2B). The limit of detection (LOD) was calculated as 5.9 aM using the equation LOD = 3.3 × (SD/S), where SD is the standard deviation of the response and S is the slope of the linear region.

Furthermore, we compared the sensitivity of our method to that of conventional RT-qPCR for the detection of SARS-CoV-2 *RdRp* RNA at various concentrations. The enhanced ThT fluorescence intensity obtained from TIGA assay with SARS-CoV-2 *RdRp* RNA was statistically significant ($P < 0.01$) at concentrations as low as 0.2 fM (Fig. 2C). RNA samples in the same concentration range (from 0.2 fM to 2 nM) were subjected to RT-qPCR, and the resulting cycle threshold (Ct) values were plotted against RNA concentration with a calculated LOD of 5.2 aM (Fig. S4). A gradual increase in Ct values with decreased concentrations of SARS-CoV-2 *RdRp* RNA showed a discerning concentration as low as 0.2 fM, with statistical significance ($P < 0.01$) (Fig. 2D). These results indicated that our system has sensitivity equivalent to that of conventional RT-qPCR for the detection of SARS-CoV-2 *RdRp* RNA.

3.4. Detection of full-length SARS-CoV-2 RNA with TIGA assay

After demonstrating the feasibility of fluorometric RNA detection based on tandem isothermal gene amplification, we applied our detection system for sensitive detection of SARS-CoV-2 full-length RNA (~30000 nt) instead of a partial gene in the SARS-CoV-2 viral RNA (i.e., *RdRp* RNA of 285 nt). 200 pM of SARS-CoV-2 *RdRp* RNA (0.5 ng) and full-length RNA (50 ng) were subjected to t-RCA, and t-RCAPs using the two RNA samples were analyzed by denaturing polyacrylamide gel

electrophoresis (Fig. S5A). The t-RCAP with high molecular weight was clearly visible in the wells of the gel, which was resistant to RNase treatment, indicating the accumulation of long stretches of ssDNA after t-RCA. Next, we performed SDA/GQ-RCA as a one-tube assay with an aliquot of each t-RCAP from SARS-CoV-2 *RdRp* RNA and full-length RNA, and monitored the enhanced ThT fluorescence signals (Fig. 3A). Background fluorescence signals were observed in the absence of target RNA (line a, Fig. 3A), whereas enhanced ThT fluorescence signals were obtained with *RdRp* RNA and full-length RNA (lines b and c, Fig. 3A, respectively). These results demonstrated that our TIGA assay can be applied for effective detection of full-length SARS-CoV-2 RNA in clinical samples.

To evaluate the sensitivity of the TIGA system for the detection of SARS-CoV-2 full-length RNA, 24 ng, 2.4 ng, and 240 pg of full-length RNA (equivalent to 100 pM, 10 pM, and 1 pM concentration, respectively, in 25 μL) were subjected to tandem isothermal gene amplification. ThT fluorescence intensity decreased as the amount of target RNA decreased (Fig. 3B). A statistically significant ($P < 0.01$) fluorescence signal was observed in samples with full-length RNA as low as 240 pg. (Fig. 3C). Additionally, our method was also compared to the conventional RT-qPCR in which SARS-CoV-2 full-length RNA (0.24, 2.4, and 24 ng) was analyzed, and Ct values were obtained (Fig. S5B). The Ct values increased as the amount of target RNA decreased, with the detection of full-length RNA as low as 240 pg ($P < 0.01$) (Fig. 3D). These results indicate that our TIGA assay has sensitivity comparable to that of conventional RT-qPCR for the detection of SARS-CoV-2 full-length viral RNA, which is mandatory in clinical environments.

3.5. Selectivity of tandem isothermal gene amplification system

To assess the selectivity of our TIGA system for the detection of target viral RNA, viral RNA from other viruses, such as HCV and influenza viruses (H1N1, H3N2, and influenza B), in addition to SARS-CoV-2, were tested. Clear, distinguishable, and bright ThT fluorescence under UV illumination was observed only in the samples containing SARS-CoV-2 full-length RNA as a target (Fig. 4A). When ThT fluorescence at 488 nm relative to the target SARS-CoV-2 RNA was estimated, the ThT fluorescent intensities of H1N1, H3N2, influenza B, and HCV were approximately 11.3%, 7.2%, 9.2%, and 4.5%, respectively (Fig. 4B). To further test the specificity of our system against SARS-CoV-2 among different types of respiratory viruses, we performed the TIGA assay for the detection of SARS-CoV-2 RNA in a mixture of non-target viral RNAs including three types of influenza viral RNA (H1N1, H3N2, and influenza B). The resulting ThT fluorescence intensity showed a linear correlation with the amount of SARS-CoV-2 RNA regardless of the presence or absence of non-target viral RNAs (Fig. 4C). Therefore, our isothermal RNA detection method based on tandem isothermal gene amplification specifically determined the presence of SARS-CoV-2 RNA with excellent distinction efficiency without interference caused by other viral genes present in the sample.

3.6. Practical applicability of tandem isothermal gene amplification system

Next, our proposed TIGA method was further applied for detection of SARS-CoV-2 positive clinical samples to verify the practical applicability. 10 clinical samples were analyzed by conventional RT-qPCR method with the cutoff Ct values of 33.5, and the analysis identified 7 SARS-CoV-2 positive and 3 negative samples (Fig. 5A). The TIGA assay was also performed with the same clinical samples, in which a group of samples (#1, #6, and #10) showed a low ThT fluorescence intensity at 488 nm similar to the RNA-free sample (No RNA) (Fig. 5B). S/B ratio 1.50 or higher was classified as SARS-CoV-2 positive with statistical significance, resulting in identification of 7 SARS-CoV-2 positive clinical samples (Fig. 5C). Thus, our TIGA assay showed perfect agreement with the conventional RT-qPCR by identifying SARS-CoV-2 positive and negative samples (Fig. 5D).

In addition, spike-and-recovery tests were conducted to assess the quantitative recovery accuracy of TIGA method as compared with conventional RT-qPCR. Calibration curve was first created by TIGA method and conventional RT-qPCR using known amount of SARS-CoV-2 full-length RNA (Figs. S6A and B). Three different amounts of SARS-CoV-2 viral RNA from clinical samples (240 pg, 2.4 ng, and 24 ng) that were spiked in diluted human plasma were subjected to TIGA assay or RT-qPCR. The amounts of the spiked RNA were determined based on calibration curve of each method (Fig. S6C). The TIGA method successfully measured the amount of SARS-CoV-2 RNA in human plasma with reproducibility and accuracy, showing the coefficients of variation (CV) less than 9.34% and the recovery rates between 97.15% and 102.13% (Table S2). In comparison, RT-qPCR method provided coefficients of variation (CV) less than 12.30% and the recovery rates between 98.17% and 107.30%. Taken together, these results demonstrated that our TIGA method is practically applicable to detect target viral RNA accurately and reliably in clinical samples.

4. Conclusions

In this study, we developed a direct detection method of SARS-CoV-2 RNA as a strategy based on isothermal tandem gene amplification without need of reverse transcription. Tandem isothermal gene amplification (TIGA) methods composed of t-RCA and SDA-coupled G-quadruplex-generating RCA (SDA/GQ-RCA) were combined to attain high sensitivity and selectivity in the SARS-CoV-2 viral RNA detection. Our method of viral RNA detection was compared with other previously reported methods for detecting viral genes in terms of viral gene sources, detection sensitivity, and viral gene amplification assay time (Table S3). The fluorometric RNA detection system based on tandem isothermal gene amplification in our study is superior to other methods and offers several advantages: ⅰ) combination of two isothermal amplification methods (RCA and SDA) in tandem provides accurate detection of viral RNA at a concentration as low as 5.9 aM (equivalent to 78 copies per assay) with a good S/B ratio of 6.9; ⅱ) viral RNA can be directly used for the assay without the need for reverse transcription and thermal cycling; ⅲ) the entire operating time for the detection of SARS-CoV-2 RNA was <1 h, with facile visualization of fluorescence signals under UV light, and ⅳ) our assay reliably showed clinical applicability in detection of viral RNA present in human plasma.

CRediT authorship contribution statement

Hyojin Lee: Conceptualization, Methodology, Validation, Formal analysis, Investigation, Writing – original draft. **Hyobeen Lee:** Conceptualization, Methodology, Investigation. **Sang-Hyun Hwang:** Resources, Investigation, Funding acquisition. **Woong Jeong:** Resources, Investigation. **Dong-Eun Kim:** Project administration, Supervision, Writing – review & editing, Funding acquisition.

Declaration of competing interest

The authors declare the following financial interests/personal relationships which may be considered as potential competing interests: Sang-Hyun Hwang reports financial support was provided by National Research Foundation (NRF) of Korea. Dong-Eun Kim has patent pending to KONKUK UNIVERSITY INDUSTRIAL COOPERATION CORP.

Acknowledgments

This research was supported by a National Research Foundation of Korea (NRF) grant funded by the Korean government (MSIT) (Grant No. 2020R1A5A1018052). This paper was written as part of Konkuk University's research support program for its faculty on sabbatical leave in 2021.

Appendix A. Supplementary data

Supplementary data to this article can be found online at https://doi.org/10.1016/j.aca.2022.339909.

References

[1] H. Li, S.M. Liu, X.H. Yu, S.L. Tang, C.K. Tang, Coronavirus disease 2019 (COVID-19): current status and future perspectives, Int. J. Antimicrob. Agents 55 (2020) 105951.

[2] C.C. Lai, T.P. Shih, W.C. Ko, H.J. Tang, P.R. Hsueh, Severe acute respiratory syndrome coronavirus 2 (SARS-CoV-2) and coronavirus disease-2019 (COVID-19): the epidemic and the challenges, Int. J. Antimicrob. Agents 55 (2020) 105924.

[3] J.B. Mahony, A. Petrich, M. Smieja, Molecular diagnosis of respiratory virus infections, Crit. Rev. Clin. Lab Sci. 48 (2011) 217–249.

[4] J.B. Mahony, Nucleic acid amplification-based diagnosis of respiratory virus infections, Expert Rev. Anti Infect. Ther. 8 (2010) 1273–1292.

[5] B. Udugama, P. Kadhiresan, H.N. Kozlowski, A. Malekjahani, M. Osborne, V.Y. C. Li, H. Chen, S. Mubareka, J.B. Gubbay, W.C.W. Chan, Diagnosing COVID-19: the disease and tools for detection, ACS Nano 14 (2020) 3822–3835.

[6] I. Smyrlaki, M. Ekman, A. Lentini, N. Rufino de Sousa, N. Papanicolaou, M. Vondracek, J. Aarum, H. Safari, S. Muradrasoli, A.G. Rothfuchs, J. Albert, B. Hogberg, B. Reinius, Massive and rapid COVID-19 testing is feasible by extraction-free SARS-CoV-2 RT-PCR, Nat. Commun. 11 (2020) 4812.

[7] D. Li, J. Zhang, J. Li, Primer design for quantitative real-time PCR for the emerging Coronavirus SARS-CoV-2, Theranostics 10 (2020) 7150–7162.

[8] J. Zhuang, J. Yin, S. Lv, B. Wang, Y. Mu, Advanced "lab-on-a-chip" to detect viruses - current challenges and future perspectives, Biosens. Bioelectron. 163 (2020) 112291.

[9] J. Yin, Y. Suo, Z. Zou, J. Sun, S. Zhang, B. Wang, Y. Xu, D. Darland, J.X. Zhao, Y. Mu, Integrated microfluidic systems with sample preparation and nucleic acid amplification, Lab Chip 19 (2019) 2769–2785.

[10] O. Tokel, F. Inci, U. Demirci, Advances in plasmonic technologies for point of care applications, Chem. Rev. 114 (2014) 5728–5752.

[11] T. Notomi, H. Okayama, H. Masubuchi, T. Yonekawa, K. Watanabe, N. Amino, T. Hase, Loop-mediated isothermal amplification of DNA, Nucleic Acids Res. 28 (2000) E63.

[12] O. Piepenburg, C.H. Williams, D.L. Stemple, N.A. Armes, DNA detection using recombination proteins, PLoS Biol. 4 (2006), e204.

[13] G.T. Walker, M.S. Fraiser, J.L. Schram, M.C. Little, J.G. Nadeau, D.P. Malinowski, Strand displacement amplification–an isothermal, in vitro DNA amplification technique, Nucleic Acids Res. 20 (1992) 1691–1696.

[14] V.V. Demidov, Rolling-circle amplification in DNA diagnostics: the power of simplicity, Expert Rev. Mol. Diagn 2 (2002) 542–548.

[15] G.T. Walker, M.C. Little, J.G. Nadeau, D.D. Shank, Isothermal in vitro amplification of DNA by a restriction enzyme/DNA polymerase system, Proc. Natl. Acad. Sci. U. S. A. 89 (1992) 392–396.

[16] X. Yan, M. Tang, J. Yang, W. Diao, H. Ma, W. Cheng, H. Que, T. Wang, Y. Yan, A one-step fluorescent biosensing strategy for highly sensitive detection of HIV-related DNA based on strand displacement amplification and DNAzymes, RSC Adv. 8 (2018) 31710–31716.

[17] B.J. Toley, I. Covelli, Y. Belousov, S. Ramachandran, E. Kline, N. Scarr, N. Vermeulen, W. Mahoney, B.R. Lutz, P. Yager, Isothermal strand displacement amplification (iSDA): a rapid and sensitive method of nucleic acid amplification for point-of-care diagnosis, Analyst 140 (2015) 7540–7549.

[18] Q. Liu, P.J. Kang, Z.P. Chen, C.X. Shi, Y. Chen, R.Q. Yu, Highly specific and sensitive detection of microRNAs by tandem signal amplification based on duplex-specific nuclease and strand displacement, Chem. Commun. 55 (2019) 14210–14213.

[19] Y. Qin, S. Liao, Y. Huang, J. Zhao, S. Zhao, Ultrasensitive fluorescent detection of nucleic acids based on label-free enzymatic-assisted cascade signal amplification, Anal. Chim. Acta 1039 (2018) 91–97.

[20] M.G. Mohsen, E.T. Kool, The discovery of rolling circle amplification and rolling circle transcription, Acc. Chem. Res. 49 (2016) 2540–2550.

[21] L. Gu, W. Yan, L. Liu, S. Wang, X. Zhang, M. Lyu, Research Progress on Rolling Circle Amplification, RCA)-Based Biomedical Sensing, Pharmaceuticals (Basel), 2018, p. 11.

[22] N.I. Goo, D.E. Kim, Rolling circle amplification as isothermal gene amplification in molecular diagnostics, Biochip J. 10 (2016) 262–271.

[23] X. Zhang, Y. Liu, Y. Yang, J. Huang, H. Wang, Z. Zhu, X. Wang, P. Ma, X. Zhou, S. Wang, X. Zhou, Ligation-promoted hyperbranched rolling circle amplification enables ultrasensitive detection of microRNA in clinical specimens, Sensor. Actuator. B Chem. 277 (2018) 634–639.

[24] X. Qi, S. Bakht, K.M. Devos, M.D. Gale, A. Osbourn, L-RCA (ligation-rolling circle amplification): a general method for genotyping of single nucleotide polymorphisms (SNPs), Nucleic Acids Res. 29 (2001) E116.

[25] H. Fujita, Y. Kataoka, S. Tobita, M. Kuwahara, N. Sugimoto, Novel one-tube-one-step real-time methodology for rapid transcriptomic biomarker detection: signal amplification by ternary initiation complexes, Anal. Chem. 88 (2016) 7137–7144.

[26] H. Fujita, Y. Kataoka, R. Nagano, Y. Nakajima, M. Yamada, N. Sugimoto, M. Kuwahara, Specific light-up system for protein and metabolite targets triggered by initiation complex formation, Sci. Rep. 7 (2017) 15191.

[27] Z. Cheglakov, Y. Weizmann, B. Basnar, I. Willner, Diagnosing viruses by the rolling circle amplified synthesis of DNAzymes, Org. Biomol. Chem. 5 (2007) 223–225.

[28] Y. Li, L. Liang, C.Y. Zhang, Isothermally sensitive detection of serum circulating miRNAs for lung cancer diagnosis, Anal. Chem. 85 (2013) 11174–11179.

[29] T. Murakami, J. Sumaoka, M. Komiyama, Sensitive RNA detection by combining three-way junction formation and primer generation-rolling circle amplification, Nucleic Acids Res. 40 (2012) e22.

[30] T. Murakami, J. Sumaoka, M. Komiyama, Sensitive isothermal detection of nucleic-acid sequence by primer generation-rolling circle amplification, Nucleic Acids Res. 37 (2009) e19.

[31] I.J. Lee, N.I. Goo, D.E. Kim, Label/quencher-free detection of single-nucleotide changes in DNA using isothermal amplification and G-quadruplexes, Analyst 141 (2016) 6503–6506.

[32] D.-M. Kim, J. Seo, D.-W. Kim, W. Jeong, S.-H. Hwang, D.-E. Kim, Fluorometric detection of single-nucleotide mutations using tandem gene amplification, Sensor. Actuator. B Chem. 314 (2020).

[33] D.-M. Kim, J. Seo, B.-H. Jun, D.H. Kim, W. Jeong, S.-H. Hwang, D.-E. Kim, Fluorometric detection of influenza virus RNA by PCR-coupled rolling circle amplification generating G-quadruplex, Sensor. Actuator. B Chem. 251 (2017) 894–901.

[34] H. Lee, D.M. Kim, D.E. Kim, Label-free fluorometric detection of influenza viral RNA by strand displacement coupled with rolling circle amplification, Analyst 145 (2021) 8002–8007.

[35] A. Petrov, T. Wu, E.V. Puglisi, J.D. Puglisi, RNA purification by preparative polyacrylamide gel electrophoresis, Methods Enzymol. 530 (2013) 315–330.